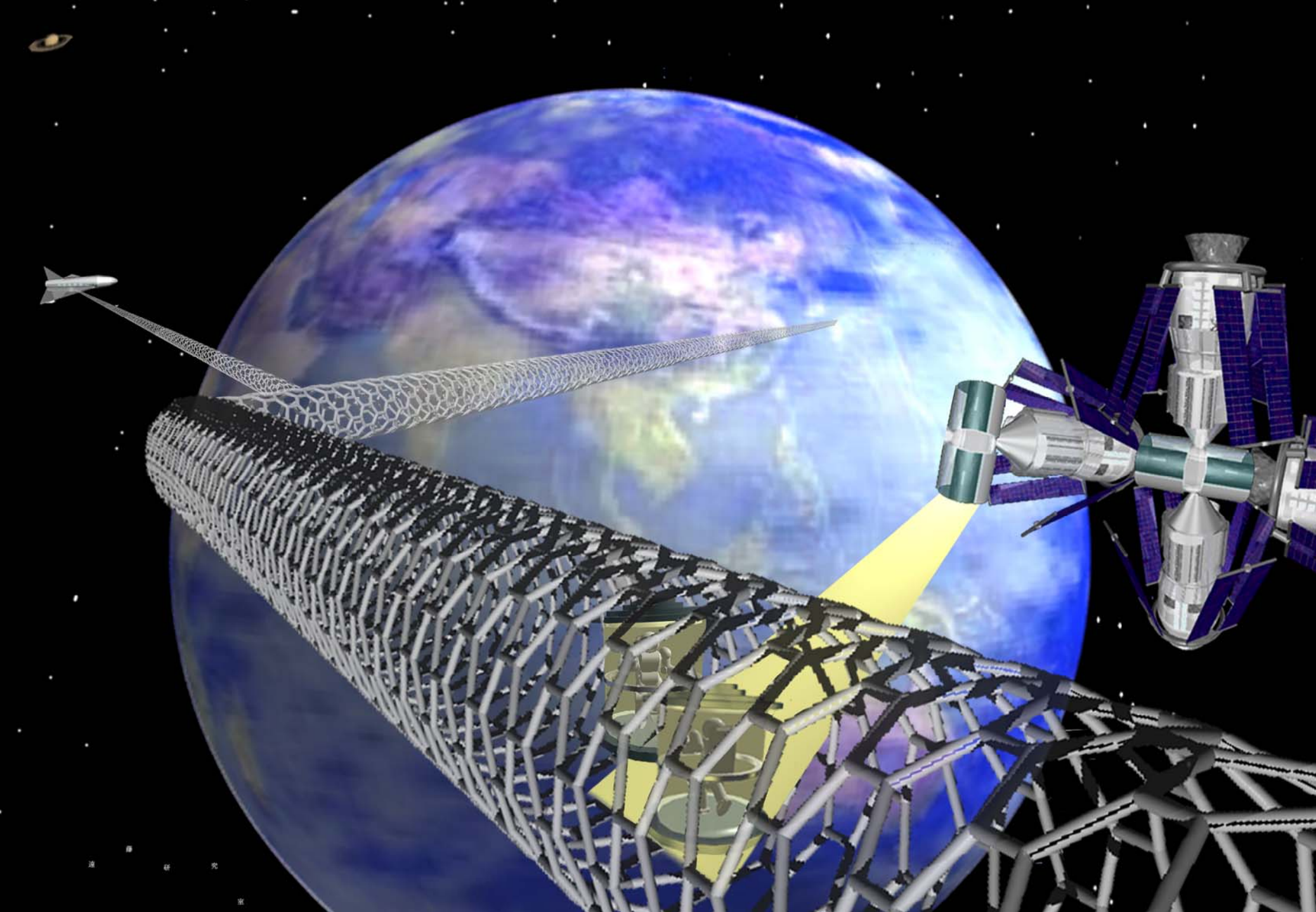

経済のサイクルと科学技術の関係；コンドラチェフのサイクル

Nikolai Dmitrijewitsch Kondratieff

(1892-1938)

Technical Revolution
Economy

Active

Stagnation

第一次産業革命

第二次産業革命

第三次産業革命

ナノテクノロジー

技術革新

1st stage

2nd stage

3rd stage

4th stage

・Steam engine
・Spinning engine

・Steelmaking method
・Radio communication
・Car
・Engine
・Air plane

・Computer
・TV
・Rocket
・Jet engine
・Atomic power
・Nylon
・Antibiotics

・Energy
・Environment
・Information, Communication
・Bio Technology

1800

1900

2000

Character of Age

The age of recent-years technical creation

The age of the basic-system establishment in the 20th century

The age of the system-technology advancement by electronics

The age of the 21st century technique

VGCF (MWCNT) obtained by Floating Reactant Method

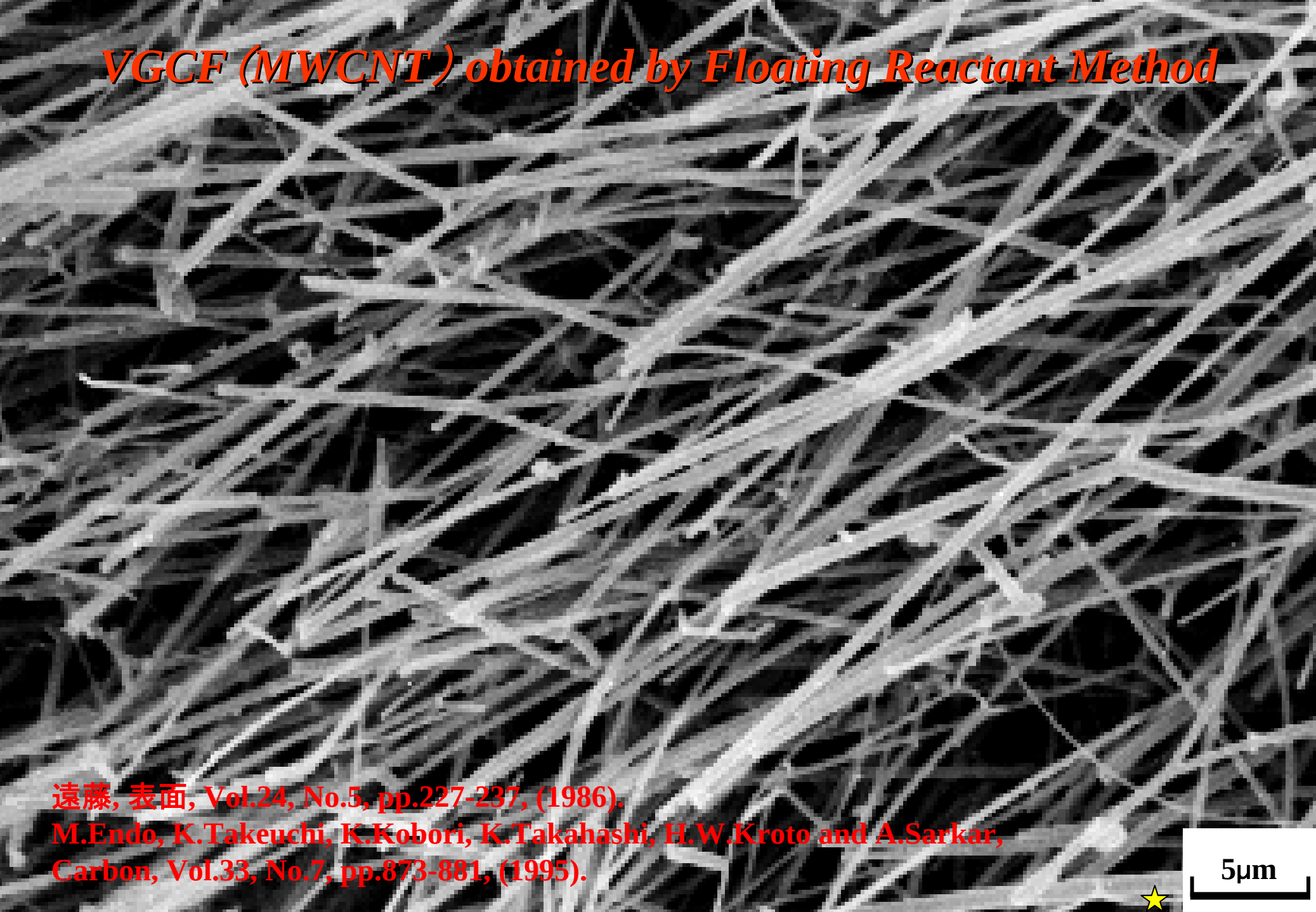

遠藤, 表面, Vol.24, No.5, pp.227-237, (1986).
M.Endo, K.Takeuchi, K.Kobori, K.Takahashi, H.W.Kroto and A.Sarkar, Carbon, Vol.33, No.7, pp.873-881, (1995).


Cross-section
of VGCF
2μm

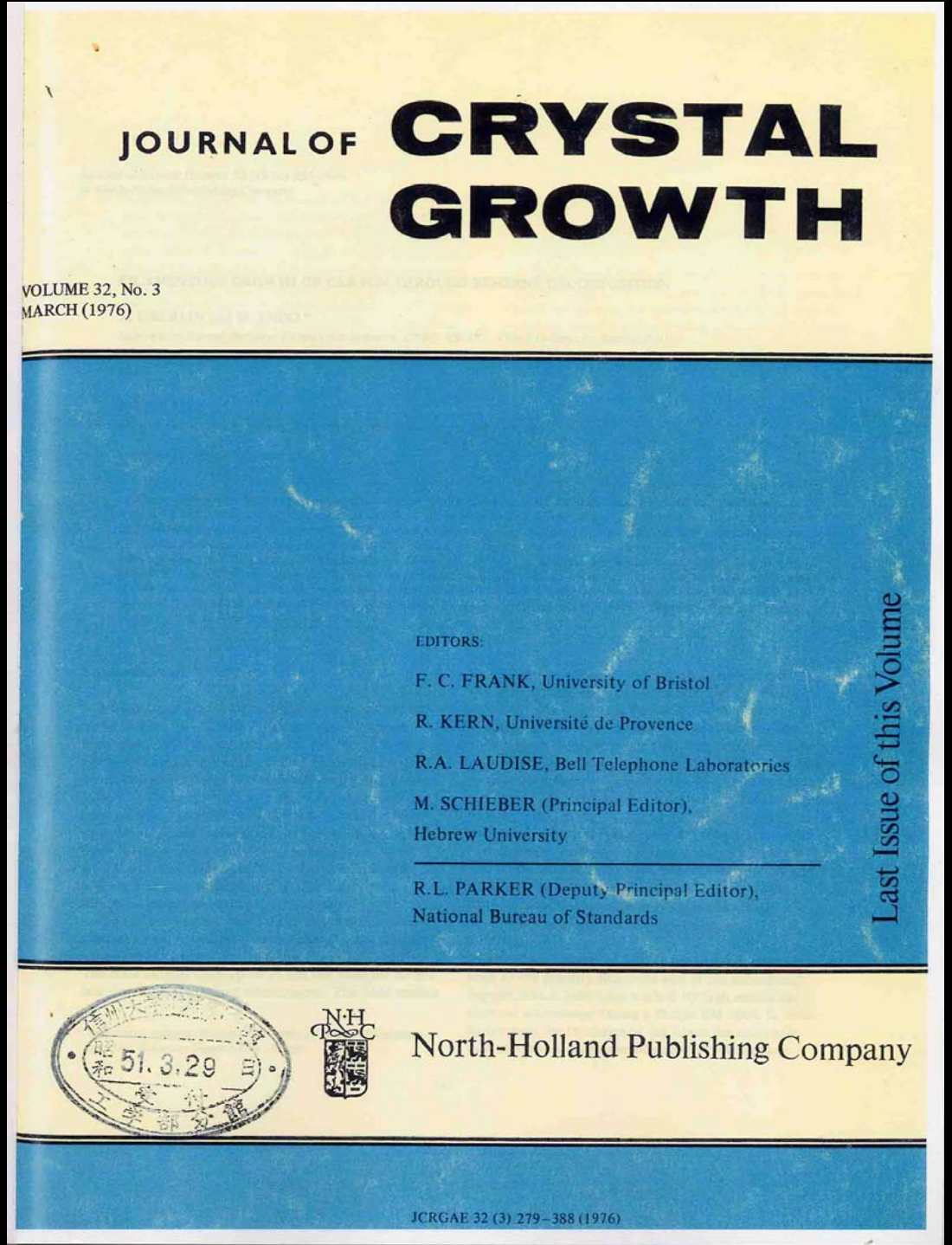

J. Cryst. Grow. 32（1976）
335-349

A. Oberlin,
M. Endo,
and
A. T. Koyama

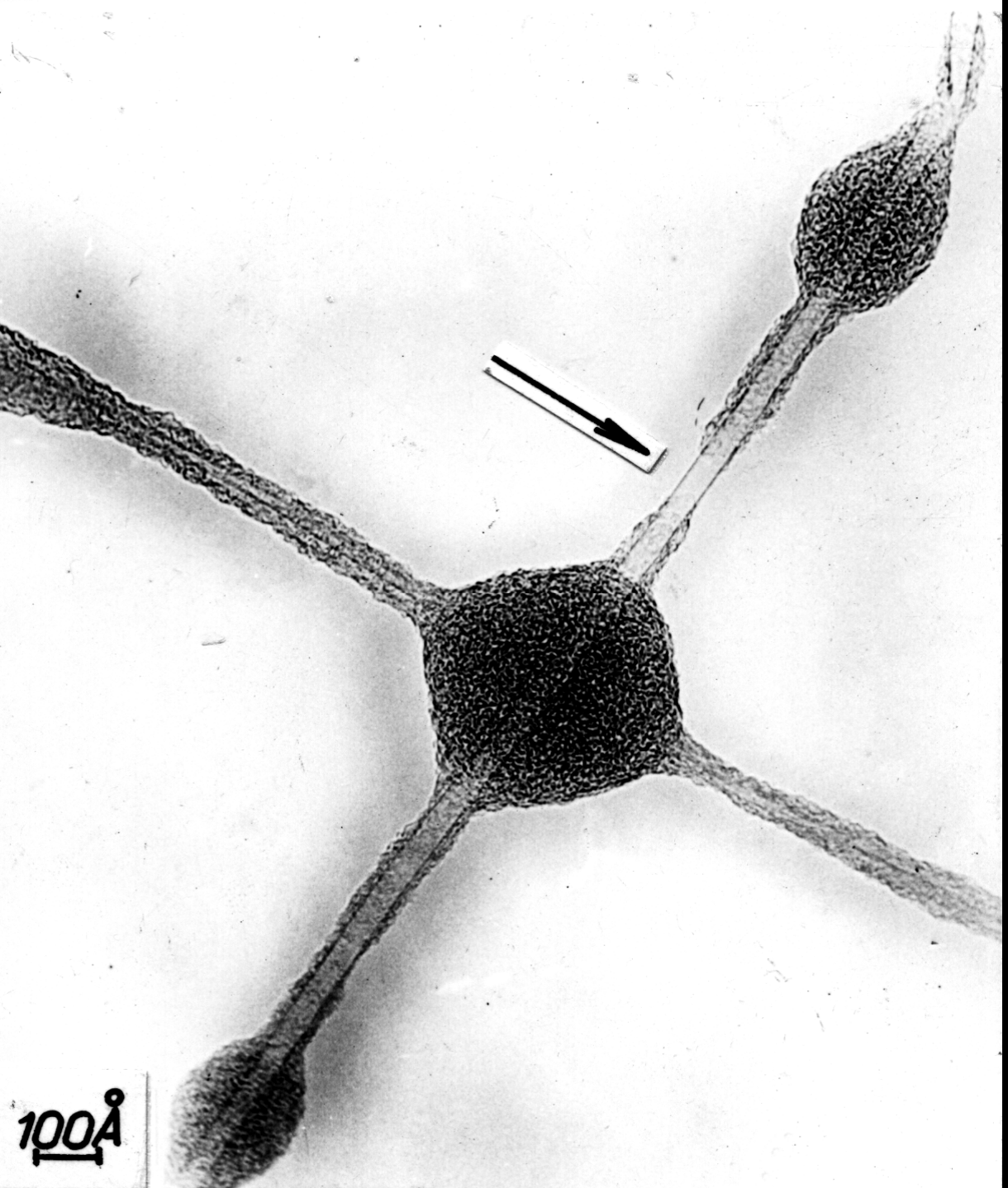

Exposed SWNT during the growth of crossing the tubes;

J. Cryst. Growth, 32（1976）335-349、
A.Oberlin, M. Endo,

and T. Koyama

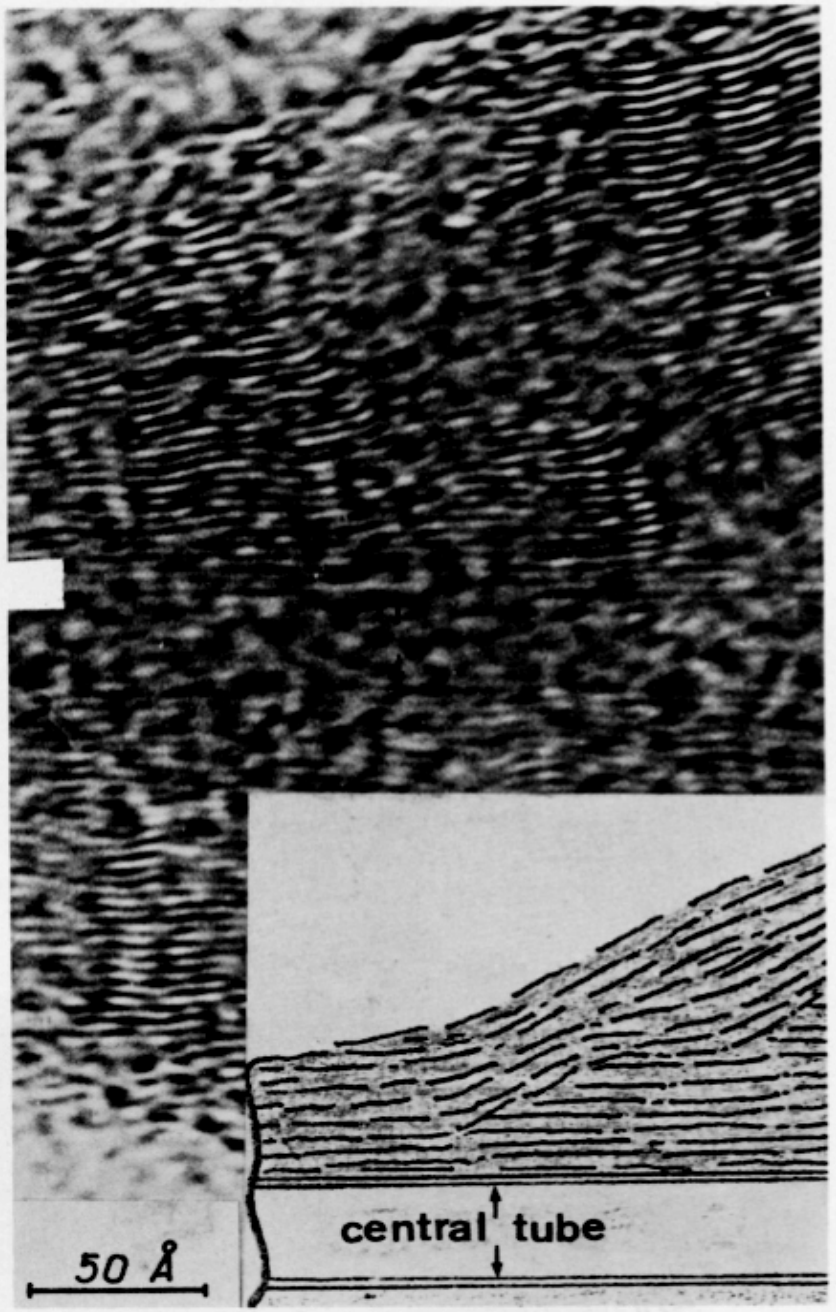

Fig. 12. (a) 00.2 lattice fringes of a constricted fibre, (b) schematic drawing of (a).

J. Cryst. Grow. 32（1976）
335-349
A. Oberlin, M. Endo,
and T. Koyama

Double layered carbon nanotube in the core of the VGCF

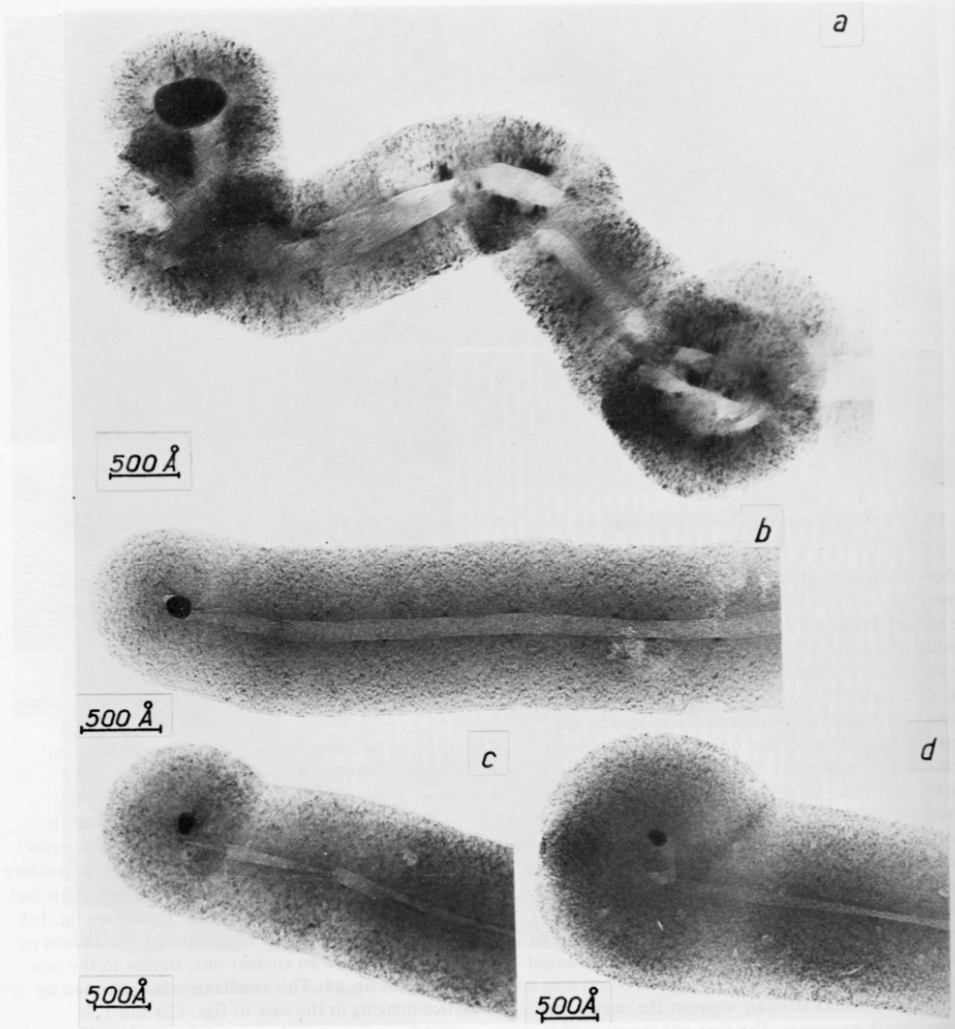

Fig. 13. Bright-field images of fibre tips showing catalyst particles.

whatever the size and shape of the fibres are, each of them contains at its tip a very small particle opaque to electrons (fig. 13). The size of these particles widely varies as it can be seen in the figure; it ranges

J. Cryst. Grow. 32（1976）
335-349

A. Oberlin,
M. Endo,
and
A. T. Koyama

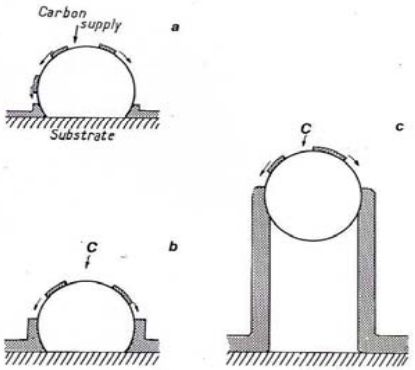

Fig. 21. Schematic illustration of fibre growth through catalytic effect.

the droplet. The carbon thus tends to nucleate on the side portions of the drop unprotected from carbon deposition because of their contact with the furnace. All these interpretations consider the diffusion of carbon atoms either through the metal or through the carbide and do not take into account any possible diffusion of metal into carbon. Moreover all of them do not really satisfactorily explain anisotropy of the growth and the occurrence of a central hollow tube.

An explanation which seems more satisfactory has been proposed by Baird et al. [26] involving a surface diffusion of "metal–metal hydrocarbon species" across the edge of the carbon layer planes. At the beginning small "liquid-like" droplets of iron get fixed on the wall of the furnace, resulting from the reduction by hydrogen of iron oxide soots. On that clean surface begins to nucleate an association of metal and hydrocarbons which diffuses on the surface and dissociates at the contact angle between the droplet and the wall of the furnace acting as a substrate. The beginning of a carbon shell is then produced. New metal hydrocarbon species dissociate on its edges and the carbon layers develop by lateral growth following the external surface of the catalyst (figs. 21a and 21b). Such a lateral growth exerts a force strong enough to lift up the catalyst particle above the surface of the substrate (fig. 21c). Layers always progress laterally in the same way and result in a filament. The hollow channel in the centre is due to the fact that no carbon supply can reach the back of the droplet, the surface of which is protected from downward surface migration by the lateral carbon layers. Growth of carbon layers would continue as long as there is a supply of metal from the top of the catalyst particle (the metal being progressively trapped between the carbon layers). When the whole droplet is covered by carbon layers at the tip, the diffusion stops and growth ends. This kind of mechanism is strongly supported by the existing relics of cementite found inside the carbon shell (see fig. 20). It must be noticed that cementite crystals are obviously formed only when cooling occurs. Such a mechanism also well explains branching of the fibres.

Increase in thickness by pyrolytic deposit on the primary thin fibres is a common phenomenon leading to graphitizable carbon. The constricted aspects often encountered at that stage of growth are probably due to the temperature gradient created along the fibre axis by a catalyst particle existing in that place. This may also be due to fluctuations of the gas flow in the reaction furnace. Anyway, such a deposit is similar to pyrolytic carbon, i.e. it is strongly oriented with its carbon layers approximately parallel to the substrate; but it is made of small turbostratic stacks with tilt and twist boundaries and thus looks more defective than the catalytic carbon contained in the core.

References

[1] W.R. Davis, R.J. Slawson and C.R. Rigby, Nature 171 (1953) 756.
[2] L.J.E. Hoffer, E. Stering and J.T. MacCartney, J. Phys. Chem. 59 (1955) 1153.
[3] L. Meyer, Z. Krist. 109 (1957) 61.
[4] M. Hillert and N. Lange, Z. Krist. 111 (1958) 24.
[5] R. Bacon, J. Appl. Phys. 31 (1960) 283.
[6] M.L. Lieberman, C.H. Hills and C.J. Miglionico, Carbon 9 (1971) 633.
[7] F.E. Wawner, Jr., J. Appl. Phys. 44 (1973) 502.
[8] T. Koyama, M. Endo and Y. Onuma, Japan. J. Appl. Phys. 11 (1972) 445.
[9] T. Koyama and M. Endo, Oyo Buturi 42 (1973) 690.
[10] T. Koyama and M. Endo, Japan. J. Appl. Phys. 13 (1974) 1175.
[11] T. Koyama, M. Endo and Y. Hishiyama, Japan. J. Appl. Phys. 13 (1974) 1933.
[12] A. Oberlin and G. Terrière, J. Microscopie 14 (1972) 1.

J. Cryst. Grow. 32（1976）
335-349

A. Oberlin,
M. Endo,
and
A. T. Koyama

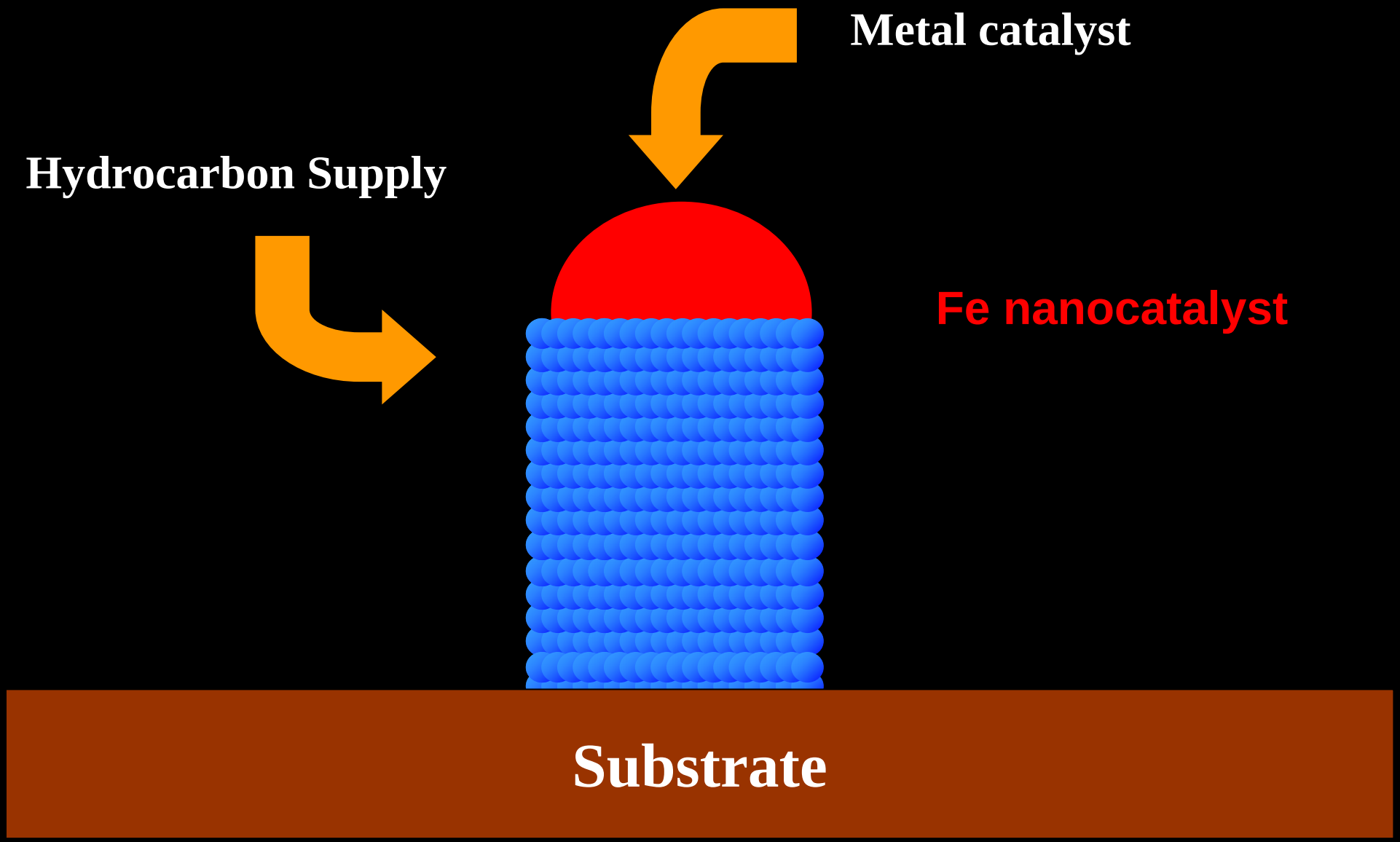

A. Oberlin, M. Endo and T. Koyama, Journal of Crystal Growth, 32, 335-349 (1976).

The Floating Seeding Method (Vertical type)

M. Endo; American Chemical Society, CHEMTECH, September, pp.568-576, (1988).

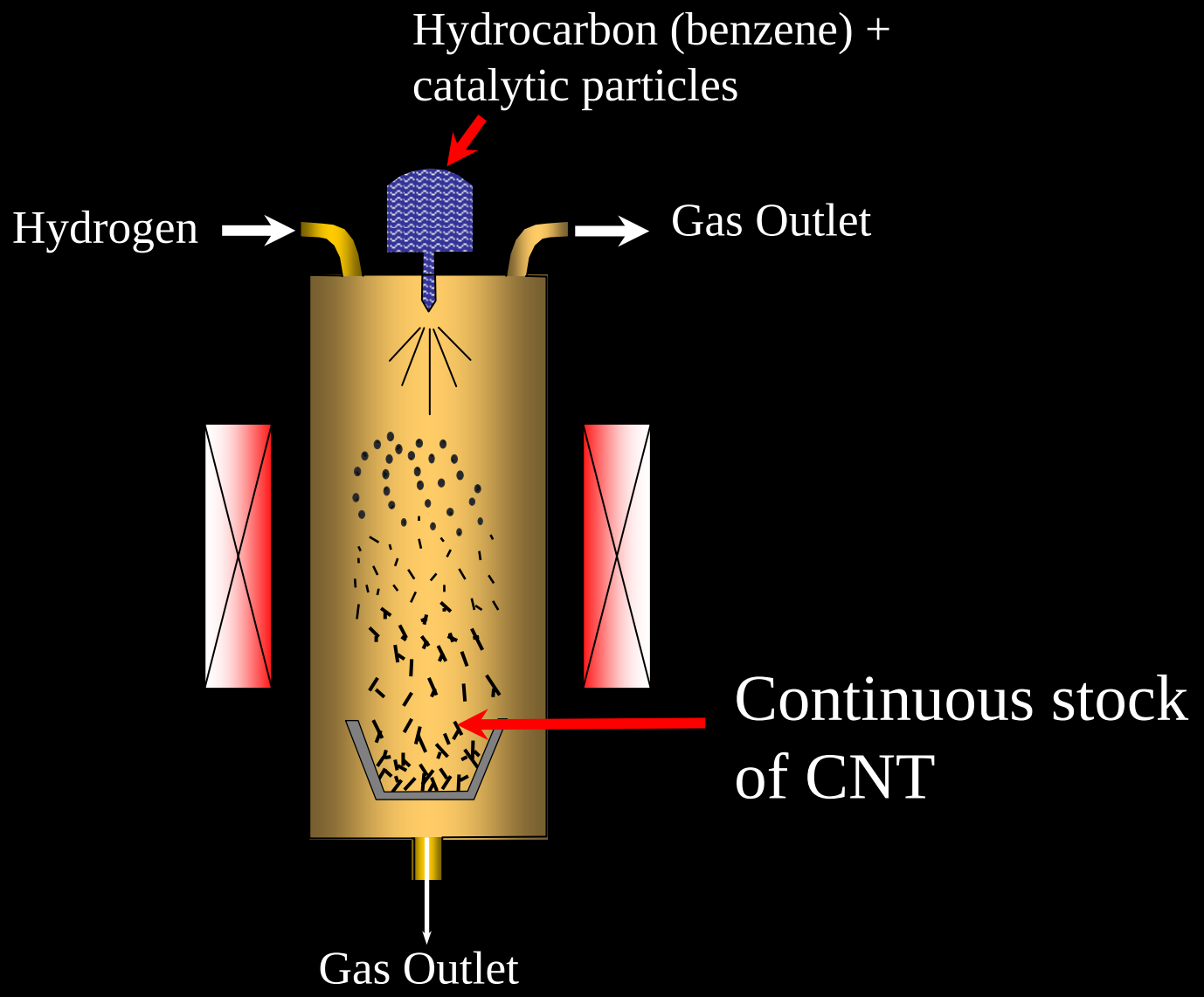

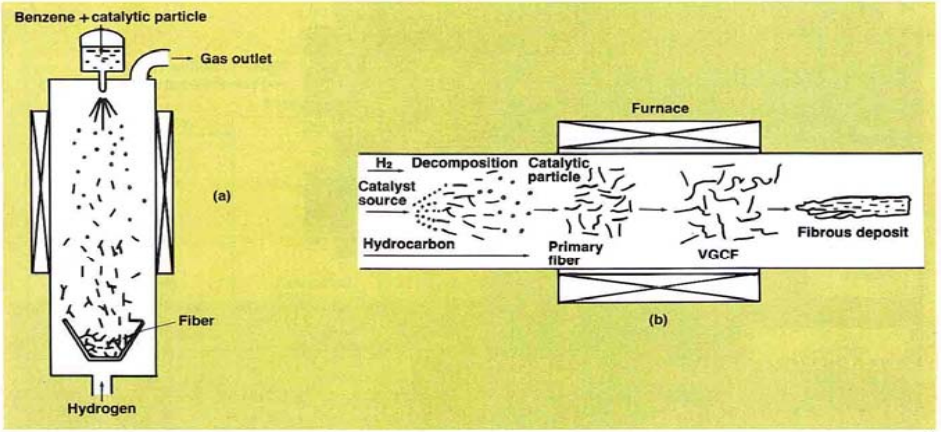

Figure 8. **Conceptual scheme of VGCF production over fluidizing catalyst particles by direct (a) and indirect (b) methods**

than those of conventional metallic or nonmetallic crystalline whiskers. This is largely due to the actions of the superfine catalyst particles.

We have developed fluidization seeding in which the initial fibers are formed over fluidized catalyst particles (Figure 8). It is much more efficient than substrate seeding for fiber formation (*9*).

Growth model and mechanism

As mentioned earlier, VGCF grows much faster than conventional whiskers, which grow at about 50 μm/s. VGCF having an aspect ratio (length/diameter) of 100 can be produced in several seconds. This ratio is equivalent to that of commercial whiskers like SiC. A reaction time of several seconds is sufficient for fine fibers to grow in a hydrocarbon atmosphere with virus-size or smaller catalyst particles. In the fluidization seeding process, the catalyst may be introduced into the reactor either directly or indirectly (Figure 8). The indirect method, by which the catalyst particles and VGCF form simultaneously, is based on Approach 3 (Figure 6). It can efficiently produce fine particles of several tens of angstroms, which, by fluidizing ultrafine metal particles introduced into the reactor in a controlled manner, greatly promotes fiber growth in the three-dimensional space of the reaction chamber. Fluidization seeding permits better control of the catalyst-feed ratio and the product aspect ratio. Fluidization-produced VGCF has a crystallographic structure similar to that of substrate-produced VGCF, but with much smaller hollow tubes of 2–3 nm (Figure 9).

It is interesting to note that the fluidization method can produce carbon fibers ranging from carbon black-like fibers with an aspect ratio of about 1 to ordinary continuous fibers, in which the aspect ratio is essentially infinite. Products having low aspect ratios can be used as reinforcing agents for various matrices, such as rubber, plastics, and cement.

Figure 10 shows the tip of a growing fiber with a crystal of iron carbide at the end of the hollow tube. The iron particle—which is either deposited on the substrate or fluidized—remains as it is while the fiber is growing but might react with the cementite particles when cooled. High-resolution transmission electron microscopy (TEM) has revealed that catalyst particles found at the fiber ends have fairly uniform sizes, mostly below 20–30 nm. Many fluidization-seeded particles are around 5 nm, which agrees with the observation that the fiber forms more efficiently with decreasing particle size. Baker and co-workers have reported that a finer particle grows the filamentous carbon faster (*10*), which may support our results for the ultrafine catalyst particles.

The fiber will continuously grow as long as the particles dispersed on the substrate or the fluidizing catalyst particles are active; the fiber ceases to grow when the particle surfaces are covered with carbon layers, oxygen, or other impurities, thus retarding movement of the carbon species. It is therefore vital to control the hydrocarbon partial pressure in the system and to keep the atmosphere free of impurities such as moisture and oxygen, in order to obtain long fibers. The TEM image (Figure 11) shows the catalyst particle at the end of the growing precursor fiber; it is not yet covered with hard, graphite-like carbon layers and can still actively assist fiber growth in the longitudinal direction. The resultant thin fibers have a continuous, thin, hollow tube as shown in Figure 11b.

We can illustrate the formation of VGCF by the model shown in Figure 12 (*11*). A reducing atmosphere of hydrogen at ~1100 °C reduces the catalyst particle of a transition metal such as iron, or cleans its surface, which promotes the polymerization and condensation of the hydrocarbon to develop hexagonal planar networks of carbon. They grow perpendicular to the substrate surface in the space between the particle and the substrate. The particle is driven upward, away from the substrate—presumably by osmotic pressure, surface tension, or

M. Endo

American Chemical Society,

CHEMTECH, September, pp.568-576, (1988).

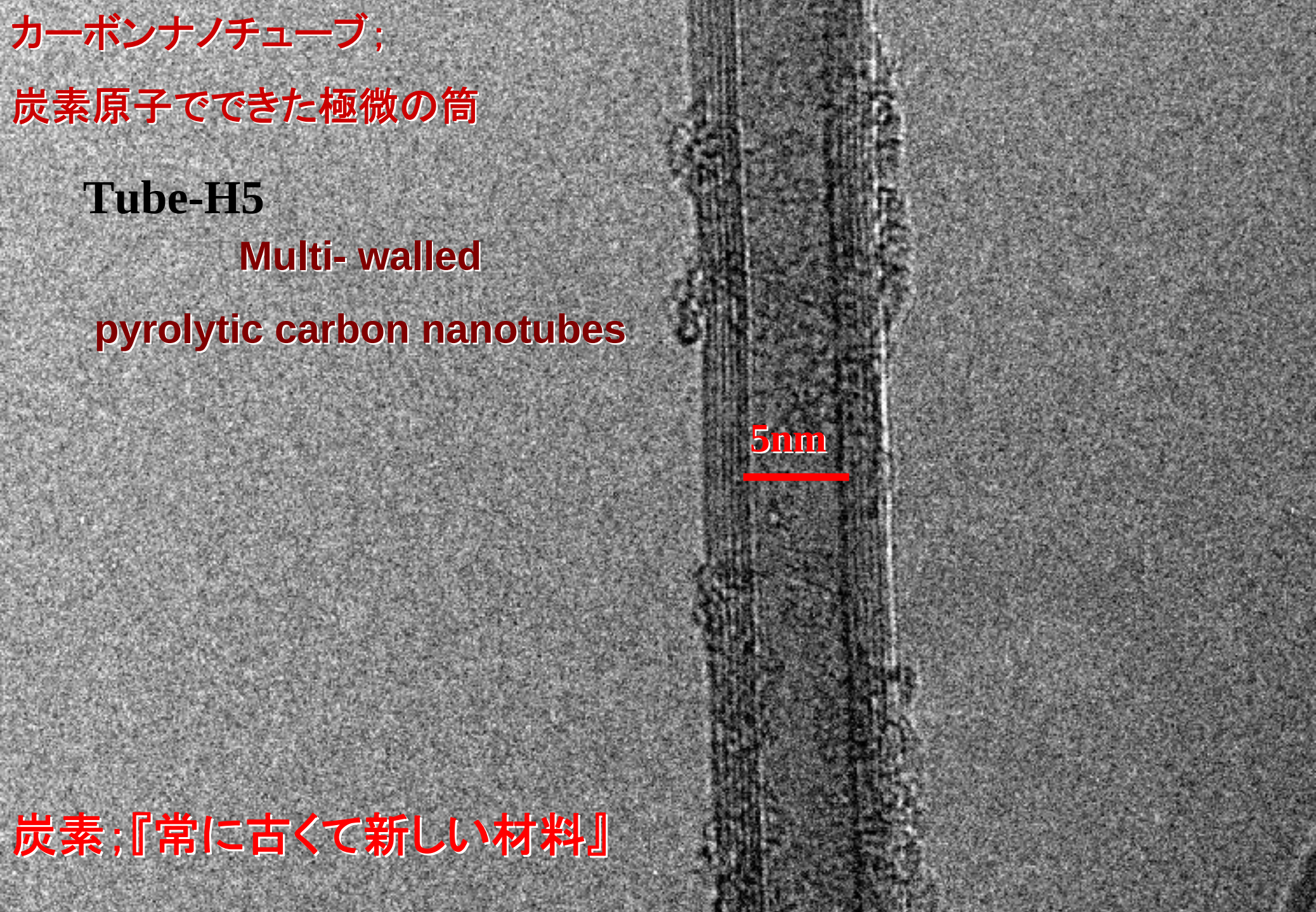
カーボンナノチューブ;
炭素原子でできた極微の筒
Tube-H5
Multi- walled
pyrolytic carbon nanotubes
5nm
炭素;『常に古くて新しい材料』

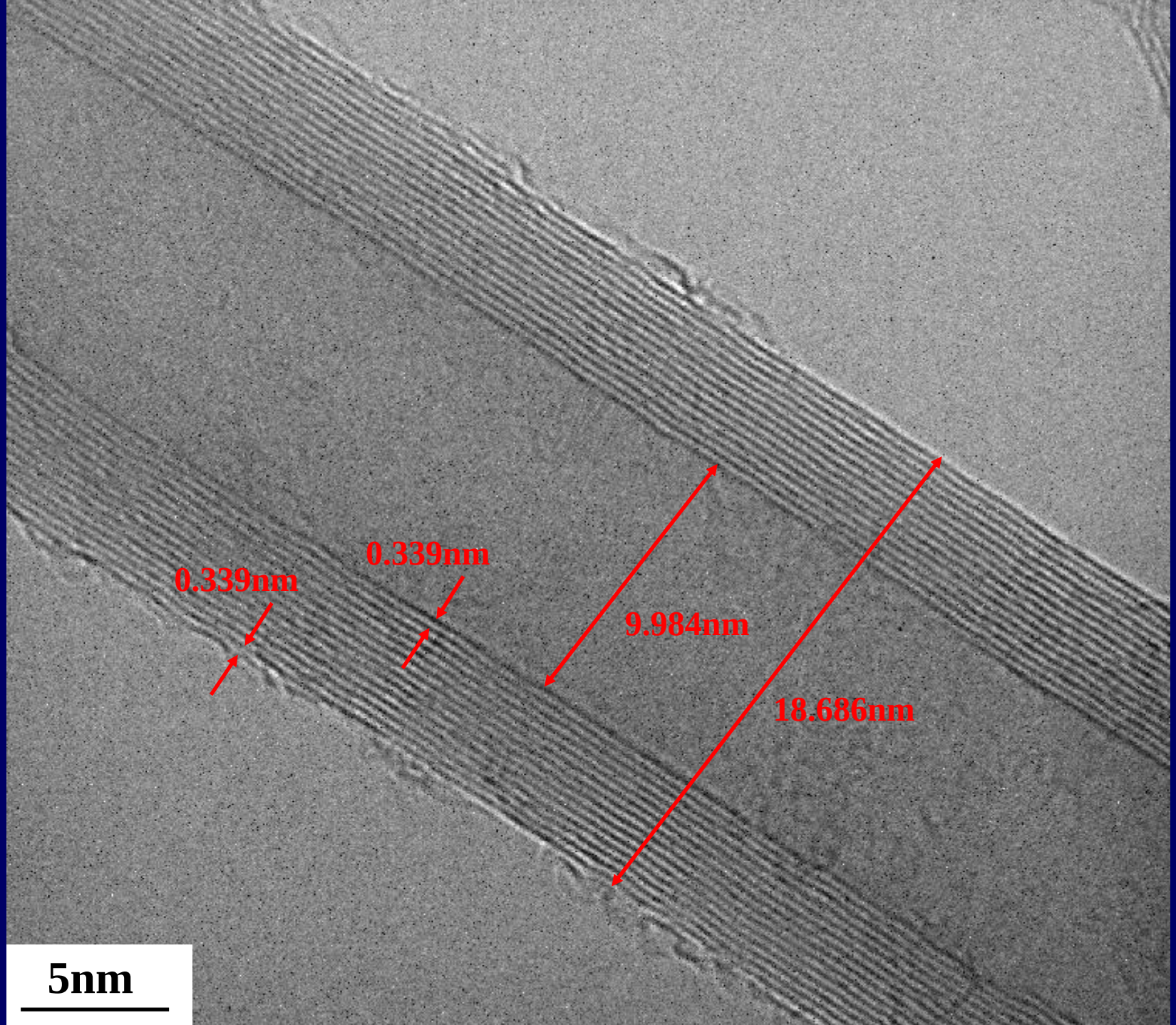
0.339nm
0.339nm
9.984nm
18.686nm
5nm

Cup-stacked CN

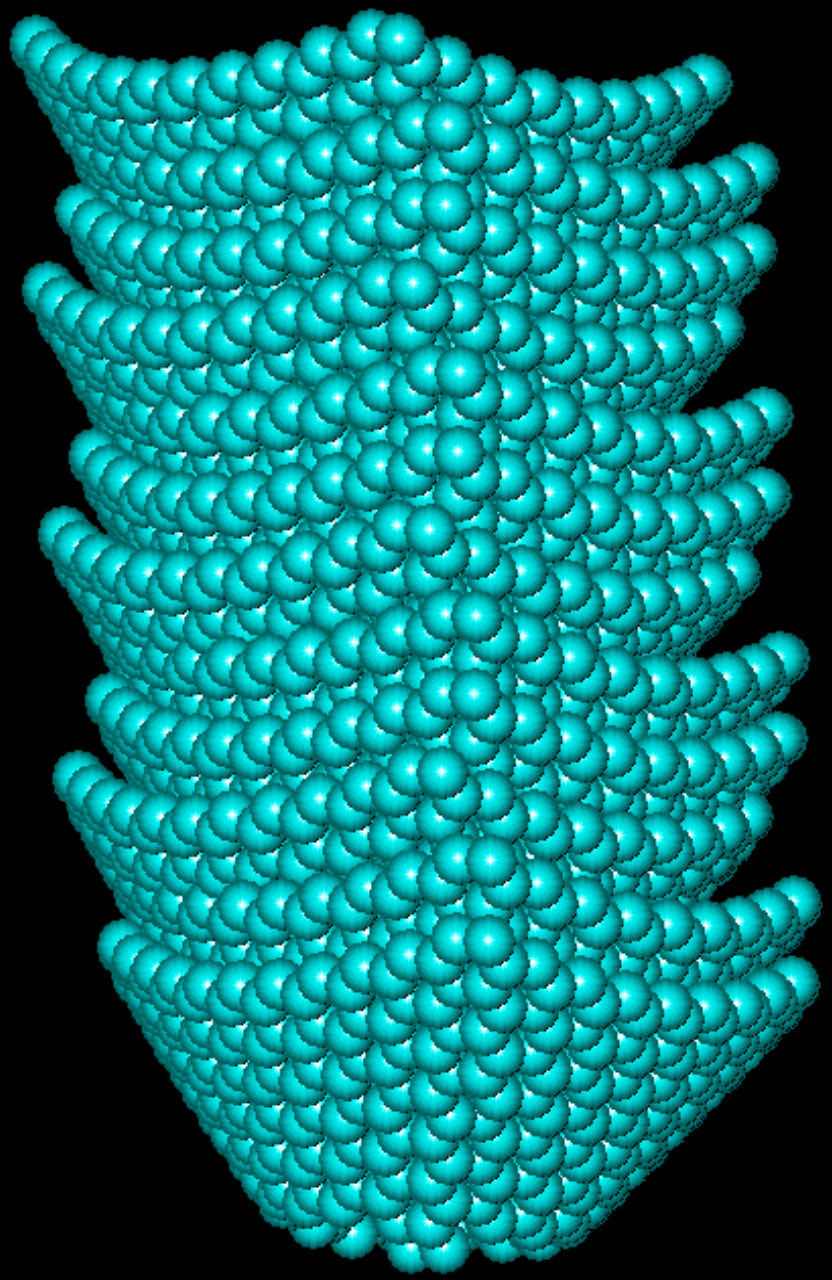

M

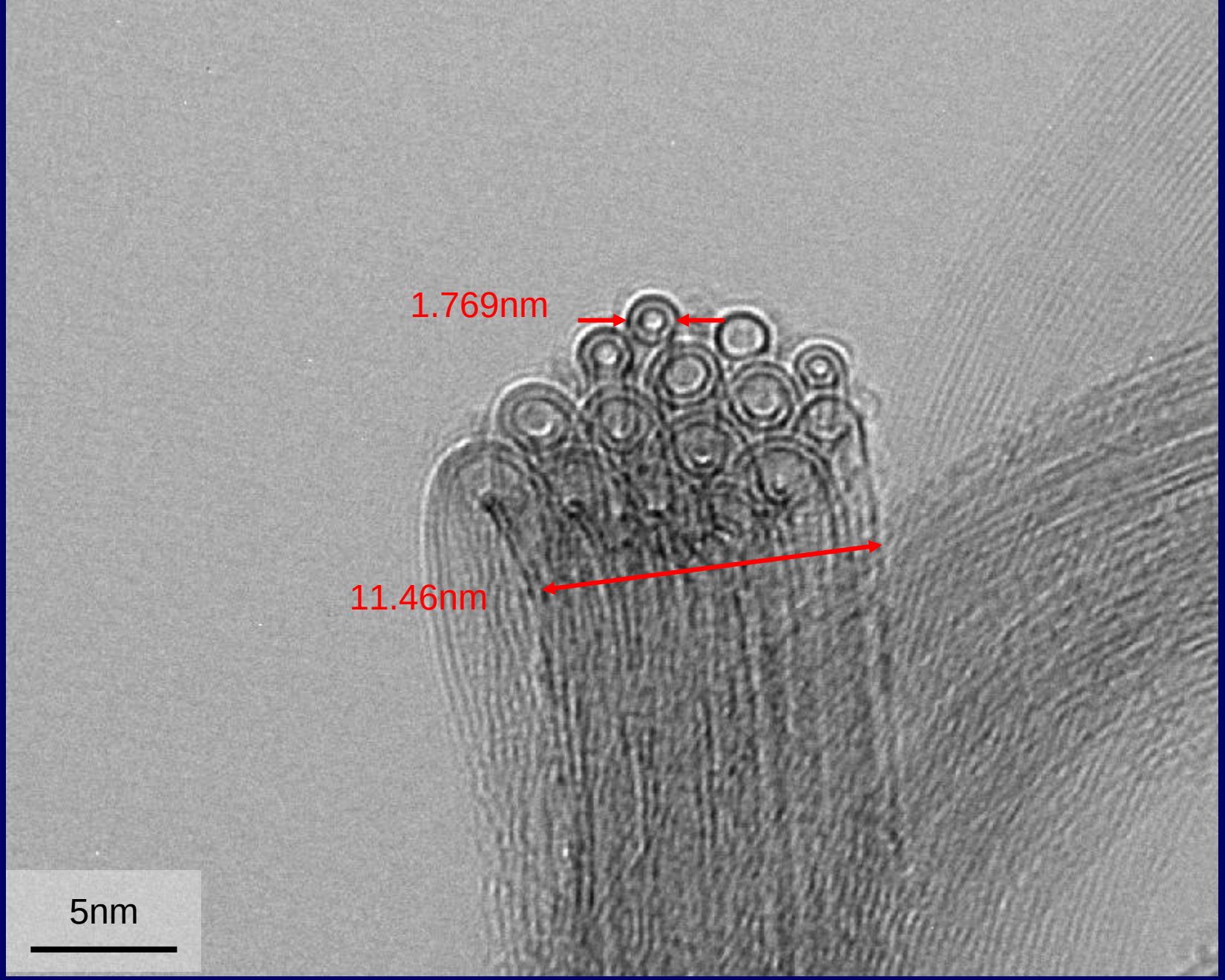

cvd-p19-51

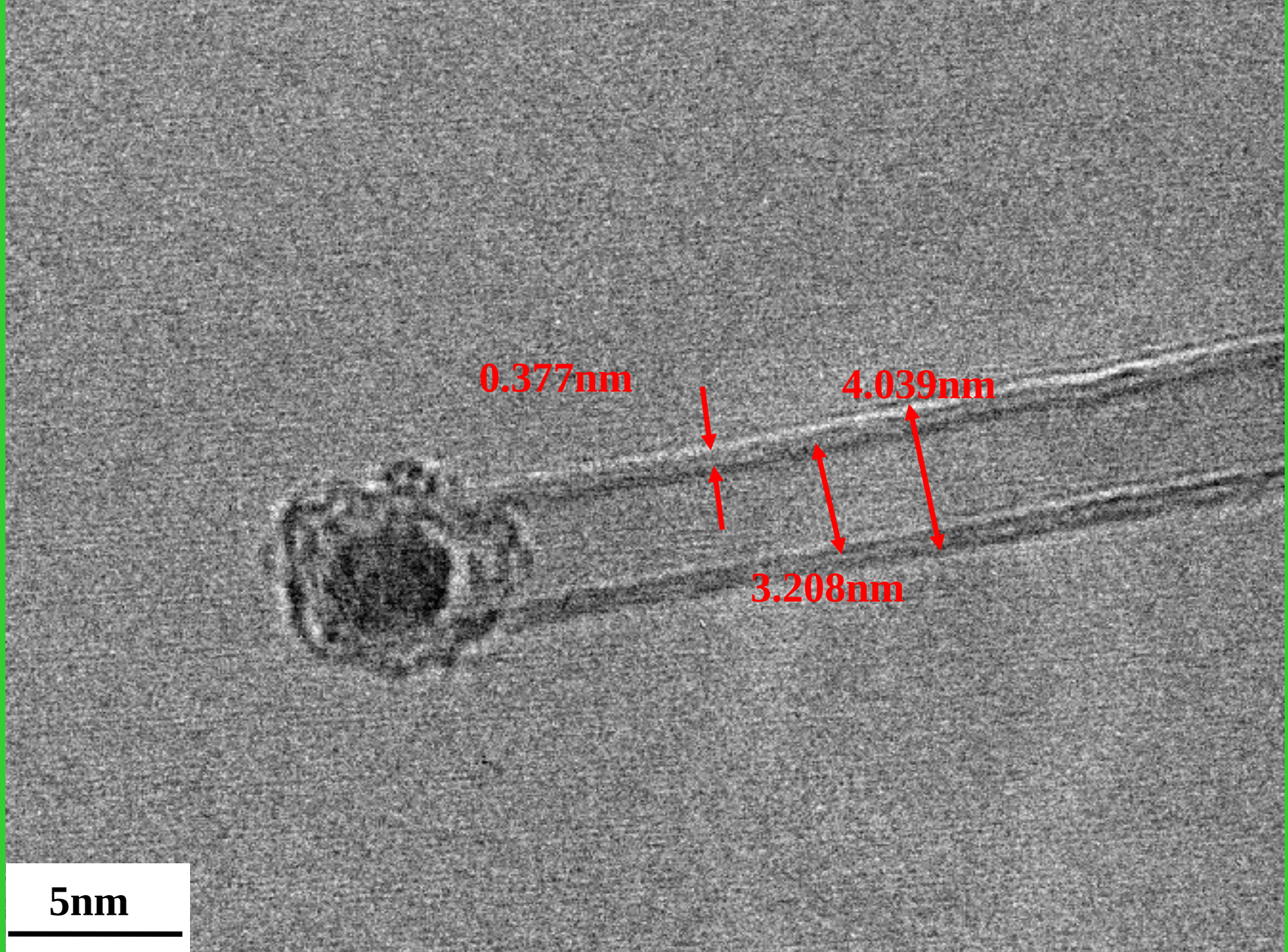
0.377nm
4.039nm
3.208nm
5nm

High purity DWNT by CCVD Method,

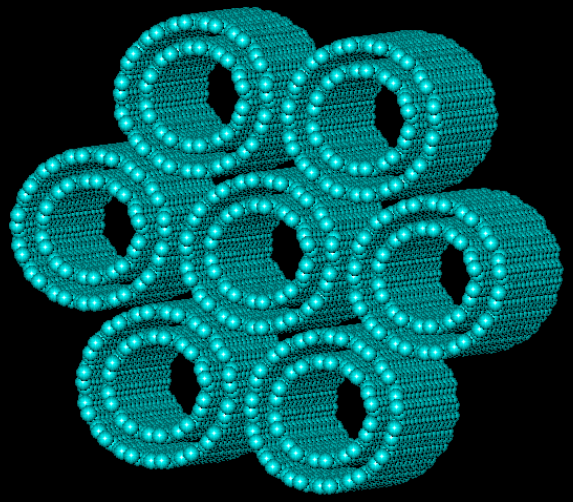

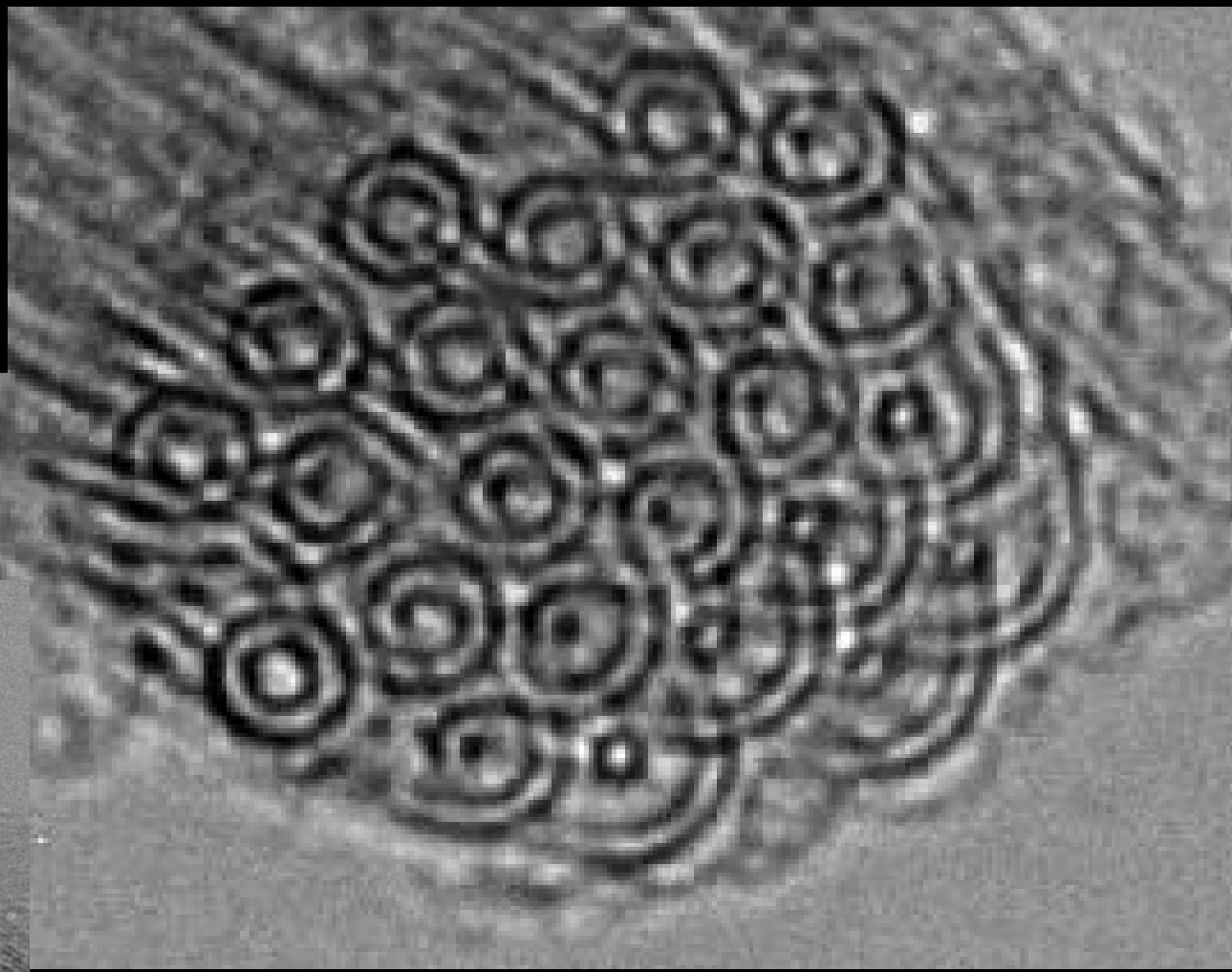

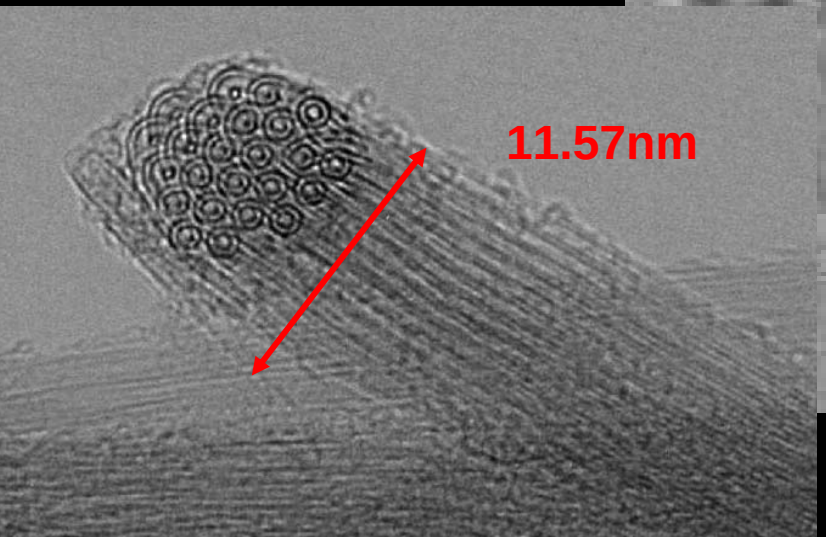

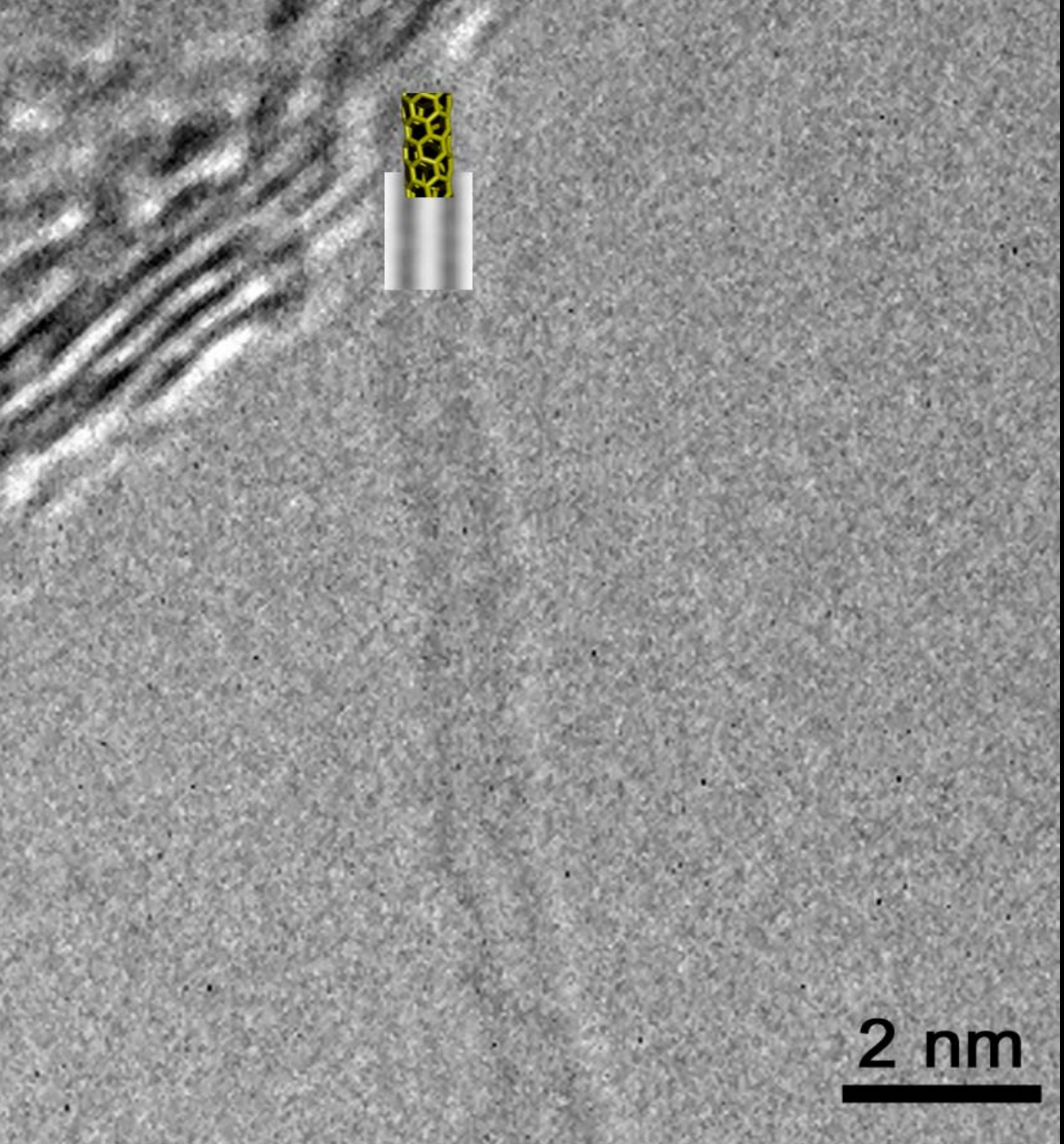

High-resolution transmission electron microscope image of a small SWNT. Inserted images are the model of (5,1) tube and the TEM simulated image, which is in good agreement with the observation.